BOARD LEVEL RELIABILITY STUDY OF NEXT GENERATION LARGE DIE WAFER LEVEL CHIP SCALE PACKAGE STRUCTURES

Timo Henttonen and Paul Mescher
Microsoft
CA, USA
timo.henttonen@microsoft.com; paul.mescher@microsoft.com

Doug Scott [1], Han Park [2], YongJae Ko [3] and Kevin Engel [1]
Amkor Technology
[1]AZ, USA; [2] CA, USA; [3]Korea
Doug.Scott@amkor.com; Han.Park@amkor.com; YongJae.Ko@amkor.co.kr;
Kevin.Engel@amkor.com

ABSTRACT
Wafer Level Chip Scale Package (WLCSP) technologies are being used more often in electronic components due to their smaller size and lower cost, and are being applied to larger die and ball matrix sizes. Originally implemented mainly in mobile devices (i.e., smartphones), WLCSP components are now frequently used in new product categories that have more stringent use conditions than the mobile space. The harsher use conditions raise a concern of solder joint reliability, especially in temperature cycling due to the difference in the coefficient of thermal expansion between the silicon die and the laminate motherboard. While cycle life can be extended by using underfill, underfilling makes the surface mount assembly process more complex and costly, increases cycle time and inhibits rework.

To solve the challenge of extending cyclic life without underfill, new WLCSP structures and materials have been proposed. This paper describes the investigation of some of these innovative solutions through motherboard assembly and board level reliability testing. The package variables consisted of two WLCSP structures utilizing ball support mechanisms and a Bismuth (Bi) bearing solder ball that is expected to increase fatigue life.

Packages were produced separately with each variable, along with legs that included both new packages and new alloy. The finished assemblies, along with a control leg of standard structure/solder, were subjected to drop testing and temperature cycling. Solder joint integrity was monitored in-situ to accurately identify duration to failure for Weibull analysis.

The results clearly show that this new generation of WLCSP structures can offer dramatically improved fatigue life without a significant sacrifice in drop reliability. This benefit should allow the use of WLCSPs in more challenging environments, as well as providing designers the option of using larger package sizes in existing mobile designs.

Key words: Wafer Level Chip Scale Package (WLCSP), board level reliability (BLR), temperature cycling, drop test, SACQ, SAC

INTRODUCTION
The Wafer Level Chip Scale Package (WLCSP) format has been developed and adopted in many different electronic component areas due to the low package cost and small size. The first WLCSP designs were developed in late 1990's for small, low pin count devices used in the mobile phone market. Since then, the package structures and solder ball alloys have evolved enormously, driven by various cost, reliability and performance requirements. The ball alloys have changed first from tin-lead (Sn-Pb) to lead-free solder, and recently to multiple tin-silver copper (Sn-Ag-Cu or SAC) alloy variations with dopants used to address drop and temperature cycling (TC) reliability challenges.

With the increased adoption rate and new application areas, pin counts have increased significantly beyond the board level reliability limit that the packages were first developed to support. Originally qualified for mobile connectivity chips with maximum 5x5-mm die size, devices including power management integrated circuits (PMIC) are now driving the die sizes well above 7x7 mm. Furthermore, these large die WLCSP devices are being used in new application areas with different and harsher use conditions compared to the traditional mobile market. This has raised concerns with the fatigue life due to the difference of coefficient of temperature expansion (CTE) between the wafer level package and the printed circuit board (PCB), which induces shear and tensile stresses and strains to the solder joints during temperature cycling.

In principal, the WLCSP design is a silicon chip with solder balls on a thin dielectric and copper redistribution layer (RDL) stack. Thus, the effective CTE of the WLCSP is

very close to silicon (3 ppm/ºC). However, the effective CTE of the PCB is much larger (typically 17 – 19 ppm/ºC with FR-4 epoxy glass multilayer laminates) but can also depend slightly on the design, structure and dielectric materials. Furthermore, there is little compliance due to WLCSP structure, small stand-off (solder joint height) and array construction. All of these factors concentrate the stresses to the solder joint interfaces and limit the size of the WLCSP that can be reliably used. Although WLCSP sizes above 49 mm^2 are currently not a substantial portion of the market space, increased reliability of larger WLCSP die would allow penetration of the package type into new device (e.g., processor) and system level (e.g., automotive, server) markets.

To extend the working size range for WLCSPs, a solution is needed to improve the temperature cycling results in board level reliability (BLR) testing without significantly sacrificing drop test performance. Several studies have shown that Bismuth (Bi) bearing alloys can extend fatigue life, but can also reduce drop test reliability [1-12].

More recently, WLCSP manufacturers have introduced changes to the structure to include mechanical locking using molding on the active side of the wafer. This molding helps decouple stress between the ball and RDL. In this study, two of these new structures were compared for reliability behavior, along with combining with Bi bearing alloys.

EXPERIMENTAL

Component Test Vehicles Description

A Design of Experiment (DOE) test matrix was constructed with five different large die WLCSP test vehicles.

WLCSP test units with daisy chain connections were designed with 7.525 x 7.525-mm die size, 18 x 18 full ball array and standard grid (no rotation), 0.4 mm ball pitch and a total of 324 balls (Figure 1). The total package thickness was 0.50 mm.

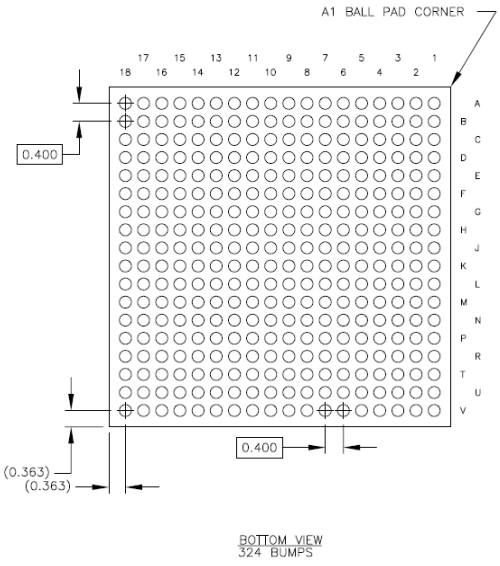

Figure 1. WLCSP test package.

The silicon size, die thickness, copper redistribution layer (RDL) with polyimide (PI) dielectric materials and under bump metallurgy (UBM) structures were kept constant in all the legs as described in Table 1.

Table 1. WLCSP test unit attributes.

Attribute	Value
Die thickness	280 µm
WLCSP technology	4-mask
RDL structure	5 µm PI / 4 µm RDL / 5 µm PI
UBM structure	8.6 µm thick Cu, no Ni/Au plating
UBM top diameter	230 µm
Raw solder ball diam.	250 µm
Ball height (pre-SMT)	198 µm

The DOE variables were the ball support structure and the solder ball alloy as listed in Table 2.

Table 2. WLCSP DOE test vehicles.

Leg #	Purpose	Ball support	Ball alloy
1	Baseline (ref.)	No	SAC405
2	Front side (FS) mold	Yes	SAC405
3			SACQ
4	5-side (5S) mold	Yes	SAC405
5			SACQ

A WLCSP ball support concept is shown in Figure 2.

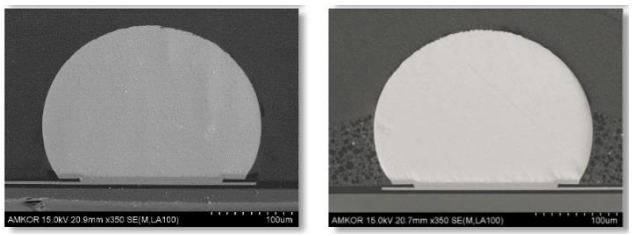

Figure 2. WLCSP structures: standard baseline (left) and ball support structure (right).

For legs 2-5 with ball support structure (FS and 5S mold), the front-side mold thickness and mold material were the same for all the legs.

Two different solder ball compositions were used, an industry standard Sn 93.5%, Ag 4% and Cu 0.5% (SAC405), and a Bismuth (Bi) doped SnAgCu alloy: Sn 92.5%, Ag 4%, Cu 0.5% and Bi ~3% (SACQ; with minor alloying elements of Ni & Ge).

For legs 4 and 5 with 5-side (5S) mold, the side wall mold thickness was 15 µm, increasing slightly the package body size to 7.555 x 7.555 mm.

A die back side lamination (BSL) protective layer of 22 µm thickness was used except in legs 4 & 5.

All test vehicles were manufactured with 300-mm wafers WLCSP assembly process in Amkor. The standard WLCSP manufacturing process flow (4-mask) is depicted in Figure 3.

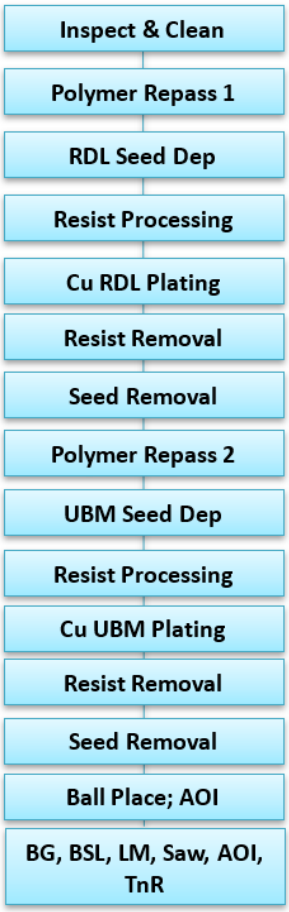

Figure 3. WLCSP manufacturing process flow.

All solder balls were included in the daisy chain net for electrical continuity monitoring during the reliability testing as shown in Figure 4.

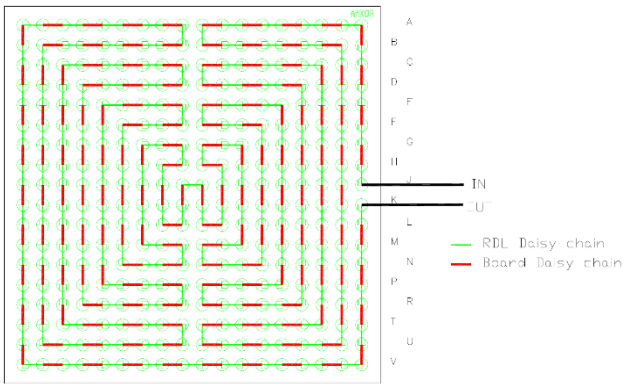

Figure 4. WLCSP daisy chain connections net.

Test Board Description

A PCB test vehicle was used in this study, with the dimensions (x,y) of 48 x 101 mm with 0.7-mm thickness. The PCB structure was 8-layer (2-4-2) build-up. The board layout was designed with 12 component locations as shown in Figure 5.

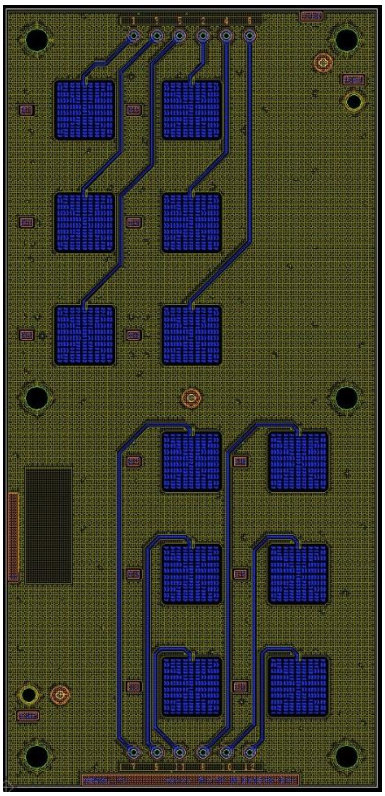

Figure 5. PCB test vehicle with 12 components layout.

The board was designed to monitor the electrical continuity of each component daisy chain individually during the reliability testing.

The PCB pad geometry for the WLCSP test vehicle was non-solder mask defined, with a 250-µm Cu pad and 300-µm solder mask opening diameter. There were no microvias on the PCB pad.

The PCB pad finish was an organic solderability preservative (OSP).

The same board design and structures were used in the accelerated temperature cycling and drop shock reliability tests.

SMT Board Assembly for Test Vehicles

All WLCSP test units were mounted to the test boards using a standard Sn 95.5%, Ag 3.8% and Cu 0.7% (SAC387), type 4.5, non-clean solder paste with 80-µm stencil thickness, and a single-pass Pb-free reflow profile (max 260°C peak temperature) with nitrogen (N_2) atmosphere.

All solder was fully melted and mixed during the reflow.

Table 3. Solder alloy liquidus temperatures.

Solder alloy	Melting point (liquidus, °C)
SAC405	225
SAC305	220
SACQ	217

The assembly and electrical test yields were 100% for all the DOE legs.

The conceptual WLCSP solder joint shapes post SMT are presented in Figure 6.

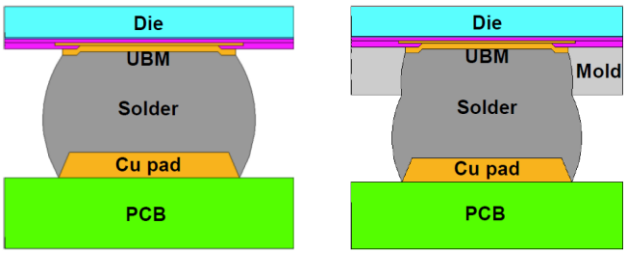

Figure 6. WLCSP solder joint shapes post SMT: standard baseline (left), and with the ball support structure (right).

A cross section analysis was carried out after SMT board assembly to verify the solder joint geometries. As expected, the DOE legs with ball support structure look different compared to the standard WLCSP (leg 1). This because of front-side mold limits the solder joint formation during the reflow process causing a 'snowman' shape as depicted in Figure 7.

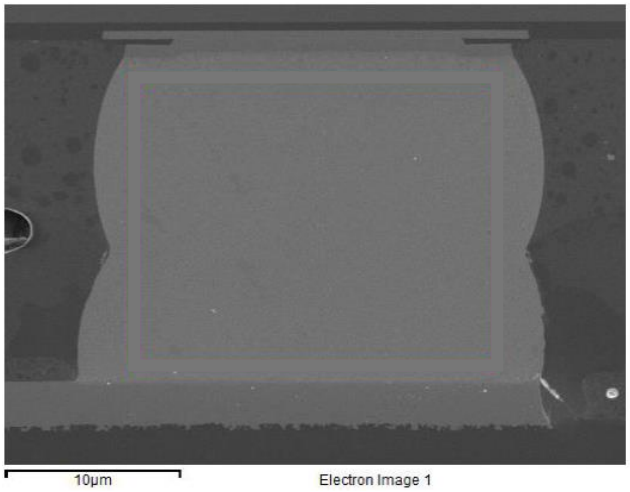

Figure 7. WLCSP solder joint shape with front-side mold ball support structure post-SMT board assembly.

On legs 2-5 (FS and 55 mold), the front side mold thickness was about half of the pre-SMT ball height.

Drop Test

Board level drop test reliability characterization was performed for all the DOE legs according to the drop test specification [13], with peak acceleration of *1500 G* and pulse duration of *1.0 ms* as depicted in Figure 8.

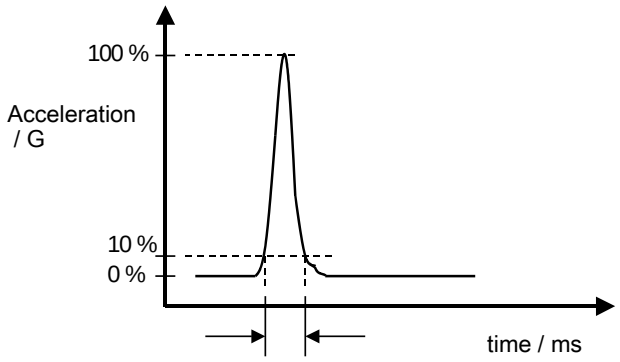

Figure 8. Drop shock test condition.

The electrical continuity of the WLCSP solder joints was monitored in-situ using an event detector. The failure criteria was defined as a resistance peak over 1500 ohms with duration longer than 1 µs.

Accelerated Temperature Cycling

The assembled test boards with WLCSP daisy chain components were subjected to accelerated TC reliability testing, with in-situ electrical continuity monitoring.

The temperature cycling test condition was according to JEDEC standard JESD22-A104, conditions G, 2, C, with a temperature range of -40 to 125°C, dwell time of 7.5 minutes at each temperature extreme, and 2 cycles per hour as shown in Figure 9.

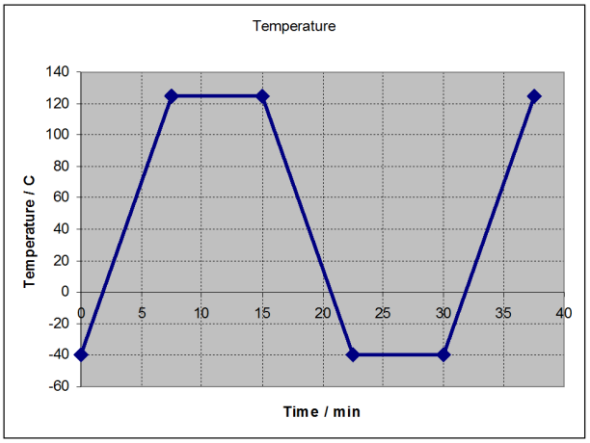

Figure 9. Accelerated temperature cycling profile.

The solder joints were monitored in-situ by using an event detector with set resistance limit of 1000 ohms and IPC-785 failure criteria.

RESULTS

Drop Test

Drop tests were performed up to 1000 drops.

The failure data was analyzed for 2-parameter (2P) Weibull statistical distribution with characteristic life (Eta) and shape (Beta) values.

The Weibull analysis results of the board level drop test reliability characterization for all the DOE legs are presented in Figure 10.

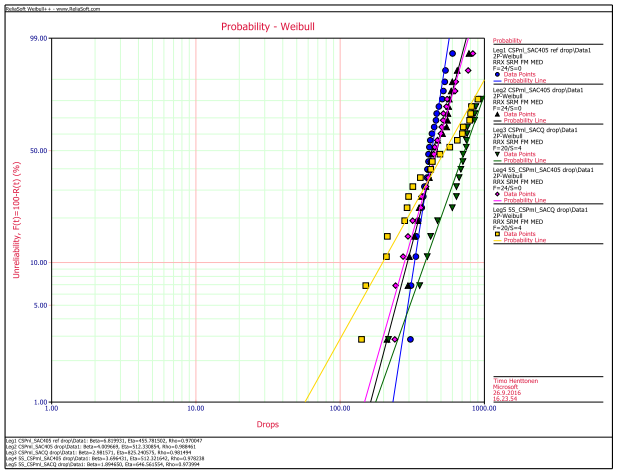

Figure 10. Weibull plot on drop test for all DOE legs.

All legs exhibited reasonably tight failure distribution, as is normally expected in drop test reliability.

Comparison of front-side mold (FS) legs compared to the baseline (reference) is shown in Figure 11.

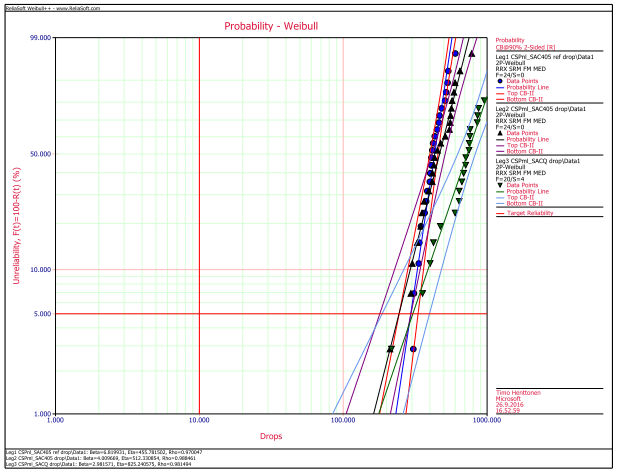

Figure 11. Weibull plot on front-side (FS) mold legs vs. baseline.

With FS mold, SACQ ball exhibited a higher reliability, whereas SAC405 ball had a similar reliability compared to baseline (SAC405 without ball support). It was rather surprising to see a higher drop test reliability with SACQ ball because it is a stiffer alloy compared to SAC405. This should be studied further in future.

Figure 12 shows the reliability of 5-sided mold (5S) legs compared to the baseline.

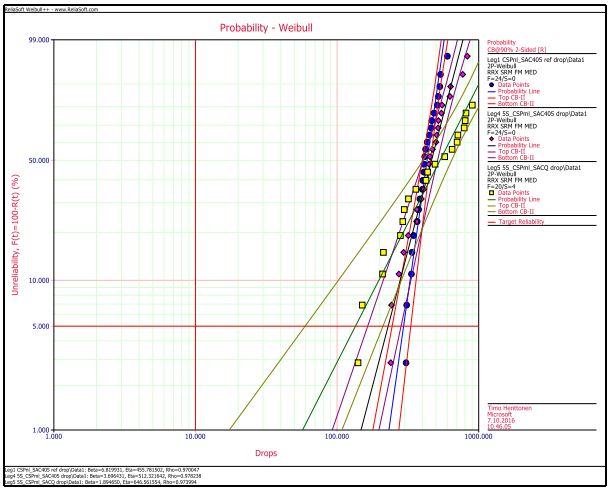

Figure 12. Weibull plot on 5-side mold (5S) legs vs. baseline.

The 5S mold did not impact the drop test reliability with the SAC405 balls. With the SACQ balls, there was more variability in drop test performance. Table 4 summarizes the drop test with 2P-Weibull parameters.

Table 4. Drop test results summary.

Leg #	Description	Beta	Eta (drops)
1	Baseline + SAC405 (ref.)	6.8	455
2	FS mold + SAC405	4.0	512
3	FS mold + SACQ	3.0	825
4	5S mold + SAC405	3.7	512
5	5S mold + SACQ	1.9	646

Failure analysis was performed by cross-section analysis and optical microscope inspection.

With leg 1 (baseline), the main failure modes were the delamination between UBM and RDL layers in the WLCSP and solder cracks at the PCB side as shown in Figure 13 and Figure 14.

Analysis on leg 2 (FS mold + SAC405 ball) showed a different failure mode and location compared to leg 1; solder fracture on the bulk solder in the snowman region and solder cracking at the PCB side, as shown in Figure 15.

Leg 3 (FS mold + SACQ ball) analysis revealed a partial delamination between UBM and RDL layers (Figure 16), and solder fractures at the PCB side.

With leg 4 (5S mold + SAC405 ball), the main failure mode was solder cracking at PCB side as depicted in Figure 17.

Cross sectioning on leg 5 (5S mold + SACQ ball) showed solder cracks in the middle of the joint in the snowman region (Figure 18) and on PCB side.

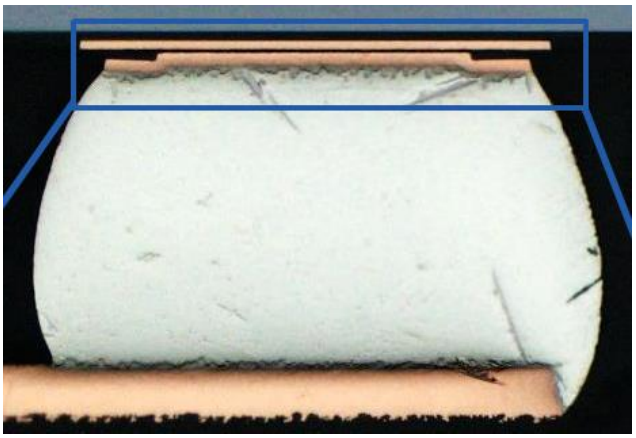

Figure 13. Leg 1 (baseline + SAC405 ball) RDL / UBM delamination.

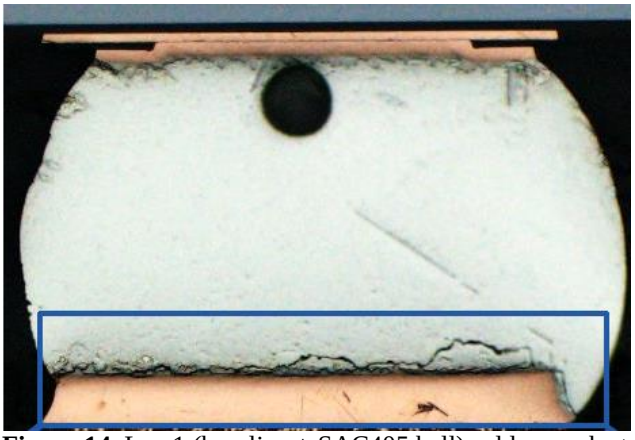

Figure 14. Leg 1 (baseline + SAC405 ball) solder crack at PCB side.

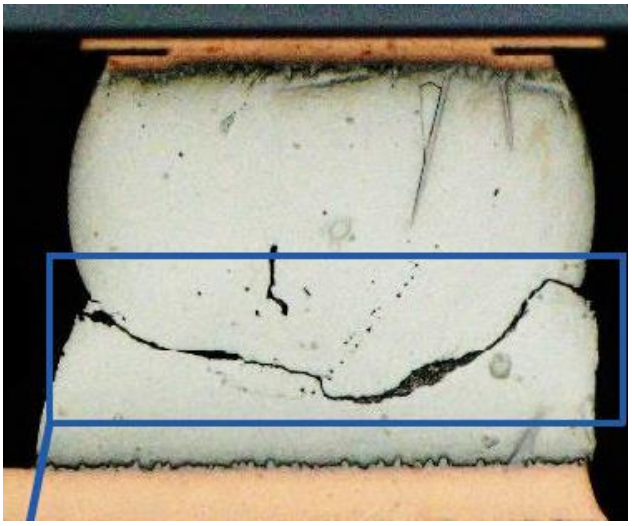

Figure 15. Leg 2 (FS mold + SAC405 ball) solder crack.

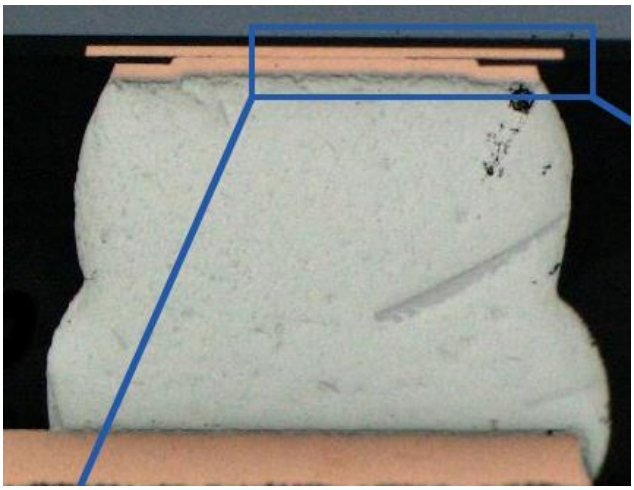

Figure 16. Leg 3 (FS mold + SACQ ball) RDL/UBM delamination.

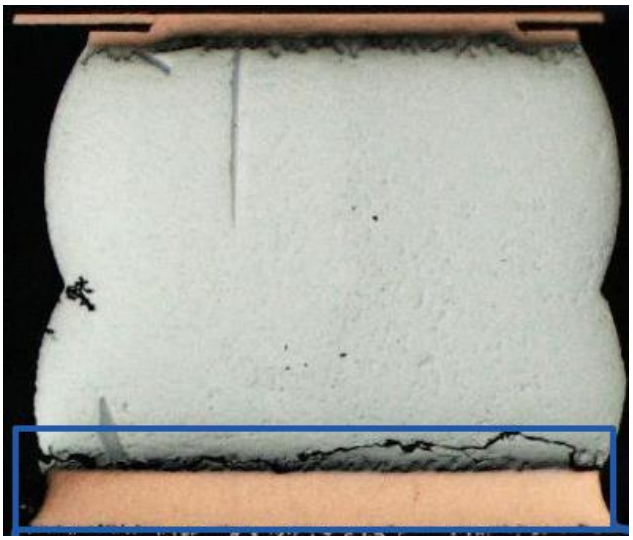

Figure 17. Leg 4 (5S mold + SAC405 ball) solder crack at PCB side.

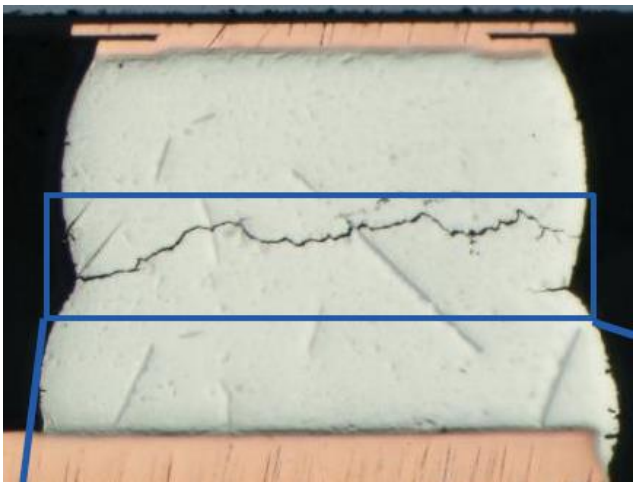

Figure 18. Leg 5 (5S mold + SACQ ball) solder crack.

Table 5 summarizes the drop test failure modes.

Table 5. Drop test failure modes.

Leg #	Description	Failure modes
1	Baseline (ref.)	RDL/UBM delamination, solder fracture at PCB side
2	FS mold + SAC405	Bulk solder fracture in the middle of the joint
3	FS mold + SACQ	Partial RDL/UBM delamination, solder fracture at PCB side
4	5S mold + SAC405	Solder fracture at PCB side
5	5S mold + SACQ	Bulk solder fracture in the middle of the joint, solder crack at PCB side

In brief, the ball support structure with SAC405 changed the failure mode from a typical RDL/UBM delamination in package toward solder cracking. In contrast, SACQ with the ball support structure showed multiple failure modes, believed to be related to the stiffer alloy changing the stresses at interfaces and within the solder joint.

Accelerated Temperature Cycling

The temperature cycling test was stopped after 3004 cycles (~3.5 months of testing).

The failure data was analyzed for 2-parameter (2P) Weibull statistical distribution with characteristic life (Eta) and shape (Beta) values.

Figure 19 shows the Weibull analysis results for all the failed DOE legs subjected to accelerated TC with -40 to 125°C profile.

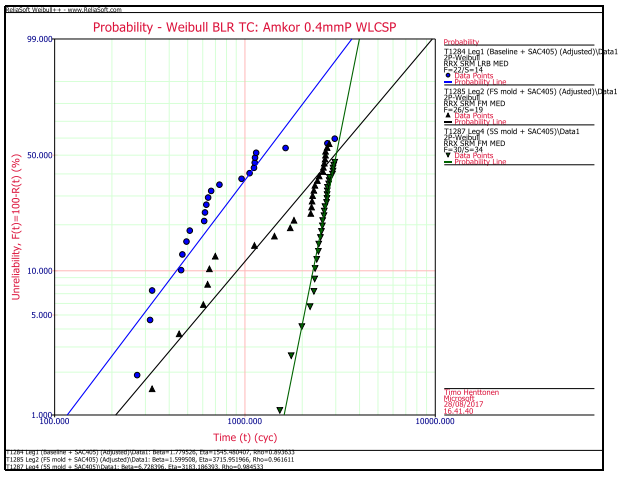

Figure 19. Weibull plot for failed legs in temperature cycling.

Failures only occurred for the SAC405 ball alloy legs.

With the SAC405 ball, both FS and 5S mold improved the temperature cycling reliability. The life cycle data indicated a *multi-modal failure distribution with FS* whereas 5S mold leg was failing more consistently. Interestingly, 5S was better than FS although they should have behaved similarly due to the ball support structure (same front-side mold thickness and material). Later failure analysis could not determine the reason(s) for reliability difference between FS and 5S legs.

For SACQ ball alloy legs, there were no electrically detectable failures with FS or 5S mold after 3004 thermal cycles.

Table 6 summarizes the accelerated TC test with 2P-Weibull parameters.

Table 6. TC test summary.

Leg #	Description	Beta	Eta (cycles)
1	Baseline + SAC405 (ref.)	1.8	1545
2	FS mold + SAC405	1.6	3715
3	FS mold + SACQ	-	-
4	5S mold + SAC405	6.7	3183
5	5S mold + SACQ	-	-

In summary, while the ball support structure (FS / 5S mold) improved the TC reliability with SAC405 solder ball, changing the solder ball alloy to SACQ with FS / 5S mold construction enhanced the TC performance to the point that failures were not able to be created.

The failure modes were analyzed by cross sectioning the selected samples.

Leg 1 (baseline + SAC405 ball) showed a classical solder fatigue cracks, as shown in Figure 20.

Leg 2 (FS mold + SAC405 ball) cross-section analysis revealed a *solder fatigue crack in the middle of the joint*, which is different to leg 1. This is due to the solder joint geometry (snowman) caused by the front-side mold limiting the joint formation during the reflow process. The analysis on the multi-modal failure distribution showed the same failure mode, a solder crack in the middle of the joint, in both units from the early and latter part of the distribution, as shown in Figure 21. Therefore, the root cause(s) the of multi-modal life data could not be determined.

Failure analysis on leg 4 (5S mold + SAC405 ball) showed a similar solder fatigue crack as leg 2.

SACQ ball legs (3 and 5) with FS and 5S mold were also analyzed although there were no observed TC test failures.

The cross-section analysis on leg 3 (FS mold + SACQ ball) found a small crack initiation in the middle of the joint (Figure 22) although it did not cause a detectable electrical failure with in-situ monitoring.

Analysis on leg 5 (5S mold + SACQ ball) revealed a small solder crack initiation in the middle region as can be seen in Figure 23.

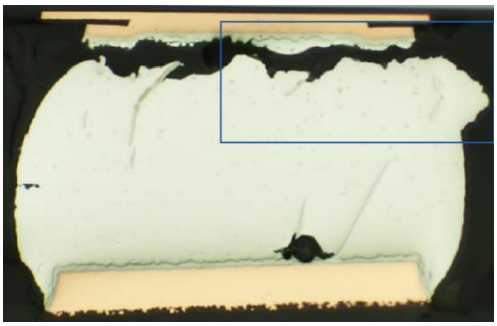

Figure 20. Leg 1 (baseline + SAC405 ball) solder fatigue crack at package side.

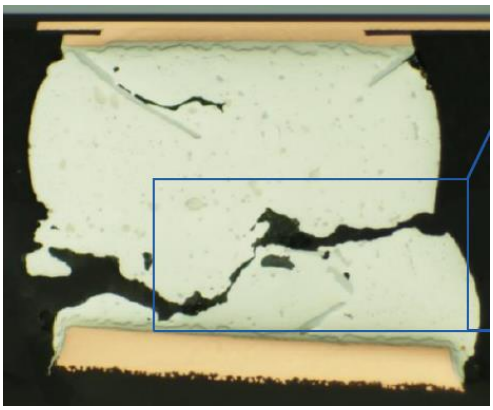

Figure 21. Leg 2 (FS mold + SAC405 ball) solder fatigue crack in the snowman region.

Figure 22. Leg 3 (FS mold + SACQ ball) post TC test.

Figure 23. Leg 5 (5S mold + SACQ ball) post TC test.

Table 7 lists TC test failure modes:

Table 7. TC test failure modes.

Leg #	Description	Failure mode
1	Baseline (ref.)	Solder fractures at package side
2	FS mold + SAC405	Solder fractures *in middle of joint*
3	FS mold + SACQ	Small solder crack initiation *in middle of joint; no electrical fail*
4	5S mold + SAC405	Solder fractures *in the middle of the joint*
5	5S mold + SACQ	Small solder crack initiation *in middle of joint; no electrical fail*

In summary, the ball support structure (FS / 5S mold) changed the failure location in solder from package side to the middle of the joint. With SACQ legs, there were no electrical continuity failures although some small solder crack initiations were observed after 3004 cycles.

CONCLUSIONS

In this study, board level reliability tests and failure analyses were performed for a large die 7.55 x 7.55-mm WLCSP. A DOE test matrix was designed for five different legs with two different variables against the baseline, namely the ball support structure and the solder ball alloy. In temperature cycling tests, the best performance was observed with a ball support structure combined with SACQ solder ball.

For the drop test, all legs showed good reliability. With the SACQ ball, FS mold improved performance, whereas with 5S mold, it introduced more variation compared to the baseline.

In conclusion, the solder fatigue life can be improved dramatically while keeping the drop test reliability at acceptable or even improved levels with the next generation WLCSP structures (FS / 5S mold + SACQ solder ball).

ACKNOWLEDGEMENTS

The authors would like to thank Alan Ton at Microsoft for the help with accelerated temperature cycling testing, Amkor Korea factory team for test components manufacturing and failure analysis, and Toptester for the performing the drop tests.

REFERENCES

[1] Pradeep Lall et al., "Thermo-mechanical reliability of SAC lead-free alloys," Proceedings of IEEE Intersociety Conference on Thermal and Thermomechanical Phenomena in Electronic Systems 2010, pp. 1 – 5.

[2] Kejun Zeng & Amit Nangia, "Thermal cycling reliability of SnAgCu solder joints in WLCSP," Proceedings of IEEE Electronics Packaging Conference (EPTC) 2014, pp. 503 – 511.

[3] Tak-Sang Yeung et al., "Material Characterization of a Novel Lead-Free Solder Material – SACQ," Proceedings of IEEE Electronic Components and Technology Conference (ECTC) 2014, pp. 518 – 522.

[4] Markus Järn et al., "Reliability Investigations of Large Die Wafer Level Packages: Optimization of Package Structure and Materials to Improve Board Level Reliability", Proceedings of Electronics System-Integration Technology Conference (ESTC) 2014, pp.1 -5

[5] Toni Mattila et al., "The Reliability of Microalloyed Sn-Ag-Cu Solder Interconnections Under Cyclic Thermal and Mechanical Shock Loading," Journal of Electronics Materials, Vol.43, No.11, 2014.

[6] Rey Alvarado, Beth Keser et al., "Study of new alloy composition for solder balls – Identifying material properties as key leading indicators toward improved board level performance," Proceedings of IEEE Electronic Components and Technology Conference (ECTC) 2015, pp. 1753 – 1757.

[7] Hikaru Nomura et al., “WLCSP CTE Failure Mitigation Via Solder Sphere Alloy,” Proceedings of IEEE Electronic Components and Technology Conference (ECTC) 2016, pp. 1257 – 1261.

[8] Chien-An Hsieh, Markus Järn et al., “Reliability Investigations of Large Die Wafer Level Packages (Part II): Impact of Solder Ball Composition, Die Thickness, and Polymer Passivation on Board Level Reliability,” Proceedings of Electronics System-Integration Technology Conference (ESTC) 2016, pp. 1 – 4.

[9] Pradeep Lall et al., “High strain rate mechanical behavior of SAC-Q solder,” Proceedings of IEEE Intersociety Conference on Thermal and Thermomechanical Phenomena in Electronic Systems (iTherm) 2017, pp. 1447 – 1455.

[10] Wei Lin et al., “SACQ Solder Board Level Reliability Evaluation and Life Prediction Model for Wafer Level Packages,” Proceedings of IEEE Electronic Components and Technology Conference (ECTC) 2017, pp. 1058 – 1064.

[11] Pei-Haw Tsao et al., “Board Level Reliability Enhancement of WLCSP with Large Chip Size,” Proceedings of IEEE Electronic Components and Technology Conference (ECTC) 2018, pp. 1200 – 1205.

[12] Md Mahmudur et al., “Characterization of material damage and microstructural evolution occurring in lead free solders subjected to cyclic loading,” Proceedings of IEEE Electronic Components and Technology Conference (ECTC) 2018, pp. 865 – 874.

[13] Esa Hussa et al., “Drop Impact Life Prediction Model for Lead-free BGA Packages and Modules,” Proceedings of EuroSIME Conference 2005.